Semi-inclusive jet functions and jet substructure in $J_{E_T}^{(I)}$ and $J_{E_T}^{(II)}$ algorithms

Lei Wang,[1] Zhong-Bo Kang,[2,3,*] Hongxi Xing,[4,5,†] and Ben-Wei Zhang[1,4]

[1]*Key Laboratory of Quark and Lepton Physics (MOE) and Institute of Particle Physics, Central China Normal University, Wuhan 430079, China*
[2]*Department of Physics and Astronomy, University of California, Los Angeles, California 90095, USA*
[3]*Mani L. Bhaumik Institute for Theoretical Physics, University of California, Los Angeles, California 90095, USA*
[4]*Guangdong Provincial Key Laboratory of Nuclear Science, Institute of Quantum Matter, South China Normal University, Guangzhou 510006, China*
[5]*Guangdong-Hong Kong Joint Laboratory of Quantum Matter, Southern Nuclear Science Computing Center, South China Normal University, Guangzhou 510006, China*

(Received 10 March 2020; accepted 3 March 2021; published 29 March 2021)

Within the framework of soft collinear effective theory, we present calculations of semi-inclusive jet functions and fragmenting jet functions at next-to-leading order for both quark- and gluon-initiated jets, for jet algorithms of $J_{E_T}^{(I)}$ and $J_{E_T}^{(II)}$ where one maximizes a suitable jet function. We demonstrate the consistency of the obtained results with the standard perturbative QCD calculations for the $J_{E_T}^{(I)}$ algorithm, while the results for fragmenting jet functions with the $J_{E_T}^{(II)}$ algorithm are new. The renormalization-group (RG) equations for both semi-inclusive jet functions and fragmenting jet functions are derived and shown to follow the timelike Dokshitzer-Gribov-Lipatov-Altarelli-Parisi evolution equations, independent of specific jet algorithms. The RG equation can be used to resum single logarithms of the jet size parameter β for highly collimated jets in these algorithms where $\beta \gg 1$.

DOI: 10.1103/PhysRevD.103.054043

I. INTRODUCTION

In high-energy proton-proton and nucleus-nucleus collisions, a tremendous number of collimated jets of hadrons are produced and measured at the Large Hadron Collider (LHC). The studies of the production rate of these jets and their substructures emerged as essential tools to probe the fundamental properties of quantum chromodynamics (QCD) [1–6] and nucleon structure [7–10]. In addition, they are also involved in searching for signals of new physics beyond the standard model [11,12], as well as in identifying the properties of the hot dense medium, quark-gluon plasma, created in heavy ion collisions [13–17]. For some recent review, see Refs. [18–20], and references therein.

Because of the crucial roles of jets, significant theoretical and experimental efforts have been devoted to the study of jets in both the particle and nuclear physics communities. For example, within the framework of soft collinear effective theory (SCET) [21–24], the cross section for inclusive jet production in pp collisions can be factorized into a convolution product of initial-state parton distribution functions f, hard-part coefficient H, and final-state semi-inclusive jet functions (SIJFs) J [25–27]:

$$d\sigma^{pp\to \mathrm{jet}+X} \sim \sum_{i,j,k} f_i \otimes f_j \otimes H_{ij}^k \otimes J_k. \tag{1}$$

The semi-inclusive jet functions J_k characterize the probability density of a parton k that is transformed to a jet. Similarly, one can also study the internal structure of the jet by measuring, e.g., the distribution of identified hadrons inside the jet, which is described by the so-called semi-inclusive fragmenting jet functions (SIFJFs) $\mathcal{G}_k^h$ [28]. The relevant factorization formula is very similar to that in Eq. (1) but replacing $J_k \to \mathcal{G}_k^h$ [26,28]. Based on this factorization formula, significant extensions and improvements are established including the study of jet quenching physics for light flavors [29] and next-to-leading order (NLO) calculations for heavy flavor jet in vacuum [30,31] and in medium [32], as well as the application to study heavy quarkonium production mechanism [33,34].

*zkang@g.ucla.edu
†hxing@m.scnu.edu.cn

In all these works, typical algorithms, for example, cone and/or anti-k_T algorithms, are used to match to the experimental analysis. The final results at NLO show single logarithmic structure $\alpha_s^n \ln^n R$ with R represents the size of the identified jets. These logarithms spoil the convergence of perturbative expansion and, thus, need to be resummed to all orders. This can be realized through the renormalization-group (RG) equations of the relevant semi-inclusive jet functions. It has been shown that such RG equations are the same as the timelike Dokshitzer-Gribov-Lipatov-Altarelli-Parisi (DGLAP) evolution equations [25,26,35].

A while ago, another type of jet algorithm was proposed initially by Georgi [36], where the idea is to cluster jets by maximizing a fixed and suitable function of the total four-momentum of jets. This algorithm was subsequently improved by Bai, Han, and Lu [37] by using the total transverse energy instead of the energy in the fixed function, which is more appropriate for hadronic collisions such as those at the LHC, because transverse energies are boost invariant. This type of algorithm has been implemented into the standard perturbative QCD (pQCD) calculations at NLO for single-inclusive jet production [38] and jet fragmentation functions [27] at hadron colliders, in which infrared safety of the algorithms is established and comparisons to cone and anti-k_T algorithms are presented. Since these algorithms maximize a suitable jet functions, we will refer to them as "*maximized jet algorithms*" for simplicity.

Although no experimental studies are currently using maximized jet algorithms, theoretical studies in understanding such jet algorithms and the associated jet observables based on such algorithms can be very beneficial. For example, in Ref. [37], the maximized jet algorithm has been studied in great detail, and a numerical code in implementing such an algorithm at the LHC has been developed. The authors found that jets constructed in this algorithm have a cone shape in Cartesian coordinates. Moreover, the size of the cone shrinks when going toward the beam direction, which effectively cuts off the beam and, thus, avoids clustering excessive particles into a single jet in the forward region. In addition, the authors found that, although many features of jets constructed in this algorithm are similar to the widely used anti-k_T algorithm, such a jet algorithm has a larger efficiency than the anti-k_T algorithm for identifying objects with hard splitting such as a boosted W jet. In another study performed in Ref. [39], the author found a surprising connection between three seemingly unrelated approaches to jet finding: the maximized jet algorithm, the 1-jettiness minimization [40–43], and the stable cone finding [44,45]. They correspond to the same meta optimization problem, whose spirit is deeply rooted in the maximized jet algorithm. Most recently, it has been shown in Ref. [46] that the maximized jet algorithm can be naturally written as a quadratic unconstrained binary optimization problem, which can then be solved via quantum annealing [47,48].

In the same spirit of theoretically exploring this jet algorithm further, in this work, within the framework of SCET, we perform explicit calculations at NLO to study SIJFs and SIFJFs in maximized jet algorithms of $J_{E_T}^{(I)}$ and $J_{E_T}^{(II)}$ [37] as defined in the next section. Although there have been calculations with the standard perturbative QCD techniques for $J_{E_T}^{(I)}$ algorithm [27,38], we demonstrate that there are interesting advantages in performing the calculations directly from the operator definitions of SIJFs and SIFJFs within SCET, and we compare our results with the standard perturbative QCD calculations. We also perform the calculations in both light-cone gauge and covariant gauge for cross-checking our results, while the previous calculations are typically performed in covariant gauge; see, e.g., [25,49]. For both SIJFs and SIFJFs, we find exactly the same divergent behavior, which leads to exactly the same RG equations, i.e., timelike DGLAP evolution equations, independent of specific jet algorithms, while the remaining finite parts exhibit the algorithm dependence. These RG equations can be used to perform the resummation of single logarithms of the jet size parameter β for maximized jet algorithms, where $\beta \gg 1$ corresponds to highly collimated jets. In this sense, the situation is very similar to the case in the anti-k_T algorithm, where the RG equations are used to resum single logarithms of the jet radius R for the narrow jets with $R \ll 1$ [25]. Note that we focus on fully analytical calculations of the SIJFs and SIFJFs at NLO in the current work, and we leave phenomenological implementations of these results in pp and AA collisions for future publications.

The remainder of this paper is organized as follows. In Sec. II, we recall the operator definition of SIJFs and give an introduction to the maximized jet algorithms. In Sec. III, we present explicit calculations of SIJFs for quark and gluon jets at NLO by considering both $J_{E_T}^{(I)}$ and $J_{E_T}^{(II)}$ maximized jet algorithms and compare them with the standard pQCD results in the literature. In Sec. IV, we extend the calculation to semi-inclusive fragmenting jet functions at NLO. We conclude our paper in Sec. V.

II. DEFINITIONS AND MAXIMIZED JET ALGORITHMS

In this section, we start by giving the definition of the semi-inclusive quark and gluon jet functions in SCET, which can be constructed from the corresponding gauge-invariant quark and gluon fields. The SIJFs are interpreted as the probability density of the parton to transform into a jet. In light-cone coordinates, they are given by the following operator definitions [25] for the quark and gluon jets, respectively:

$$J_q(z, E_\mathrm{J}) = \frac{z}{2N_c}\mathrm{Tr}\left[\frac{\bar{\not n}}{2}\langle 0|\delta(\omega - \bar{n}\cdot\mathcal{P})\chi_n(0) \times |JX\rangle\langle JX|\bar{\chi}_n(0)|0\rangle\right], \quad (2)$$

$$J_g(z, E_\mathrm{J}) = -\frac{z\omega}{2(N_c^2-1)}\langle 0|\delta(\omega - \bar{n}\cdot\mathcal{P})\mathcal{B}_{n\perp\mu}(0) \times |JX\rangle\langle JX|\mathcal{B}^{\mu}_{n\perp}(0)|0\rangle, \quad (3)$$

where $E_\mathrm{J} = zE$ is the jet energy, E is the energy of the parton initiating the jet, $\mathcal{P}$ is the label momentum operator, and the state $|JX\rangle$ represents the final-state observed jet J and unobserved particles X. χ_n and $\mathcal{B}_{n\perp\mu}$ are gauge-invariant n-collinear quark and gluon fields, respectively. Note that the light-cone vector n^μ is defined along the jet axis, and its conjugate vector is $\bar{n}^\mu$. In the frame where the jet has no transverse momentum, we can write $n^\mu = (1,0,0,1)$ and $\bar{n}^\mu = (1,0,0,-1)$, which satisfies $n^2 = \bar{n}^2 = 0$ and $n\cdot\bar{n} = 2$. In such a frame, we define $\omega = \bar{n}\cdot P$ and $\omega_\mathrm{J} = \bar{n}\cdot P_J$ as the large light-cone components of the momenta for the parton initiating the jet (P) and the jet itself (P_J), respectively. For a collimated jet, we have $\omega \approx 2E$ and $\omega_\mathrm{J} \approx 2E_\mathrm{J}$.

In this work, we neglect the nonperturbative hadronization effect and consider only the perturbative aspect of the jet functions; thus, one can calculate both quark- and gluon-initiated jets perturbatively. At leading order (LO) in which one parton forms the jet, the jet functions are independent of specific jet algorithms and are simply delta functions:

$$J_q^{(0)}(z, E_\mathrm{J}) = J_g^{(0)}(z, E_\mathrm{J}) = \delta(1-z), \quad (4)$$

where the superscript (0) denotes the LO result.

At NLO, one has to consider the phase space constraints for the radiated parton according to specific jet clustering algorithms. It is this constraint that leads to the algorithm dependence of the jet functions. There are so far two classes of broadly defined algorithms: cone algorithms [44] and successive recombination algorithms [50]. Cone algorithms include the Snowmass and SIS cone algorithms [45], while recombination algorithms include the Cambridge-Aachen, k_T, and anti-k_T algorithms [51,52]. In Refs. [25,53], the semi-inclusive jet functions in cone and anti-k_T algorithms have been calculated up to NLO. In the present paper, we will extend the calculation to two other jet finding methods $J_{E_T}^{(I)}$ and $J_{E_T}^{(II)}$ [36,37], in which the primary idea is based on maximizing a fixed function of the total four-momentum of the final-state particles. Following Ref. [36], one defines one such function—the $J_{E_T}^{(I)}$ function—as follows:

$$J_{E_T}^{(I)}(P^\mu_\mathrm{set}) \equiv E_\mathrm{set} - \beta\frac{m^2_\mathrm{set}}{E_\mathrm{set}} = E_\mathrm{set}\left[1 - \beta\frac{m^2_\mathrm{set}}{E^2_\mathrm{set}}\right]. \quad (5)$$

Here, E_set and P^μ_set are the total energy and four-momentum, respectively of a given subset of the final-state particles, and m_set is its invariant mass; i.e., $P^2_\mathrm{set} = m^2_\mathrm{set}$. Reference [37] improves the above definition by using the transverse energy defined as $(E^\perp_\mathrm{set})^2 \equiv P^2_\perp + m^2_\mathrm{set}$ instead of the energy E_set, where $P_\perp$ is the magnitude of the transverse momentum. Thus, we have the $J_{E_T}^{(I)}$ function as

$$J_{E_T}^{(I)}(P^\mu_\mathrm{set}) \equiv E^\perp_\mathrm{set}\left[1 - \beta\frac{m^2_\mathrm{set}}{(E^\perp_\mathrm{set})^2}\right]. \quad (6)$$

Apparently, the definition in Eq. (5) is more suitable for jet production in e^+e^- collisions where the energy of the jet is relevant. On the other hand, the definition in Eq. (6) uses transverse energies which are boost invariant and, hence, more suitable for the application to hadronic scattering, such as pp collisions at the LHC. Note that, for collimated jets, the so-called narrow jet approximation (NJA) applies, and one could replace the transverse energies $E_\perp$ by the transverse momenta $P_\perp$. In our calculations below, we choose a frame in which the jet has zero transverse momentum, and, thus, we will follow Eq. (5) in most of our calculations. However, once our calculations is done, translating from Eq. (5) to Eq. (6) will correspond to simply replacing the jet energy E_J in our final expressions by the jet transverse momentum $P_{\mathrm{J}\perp}$ for studying jet production in pp collisions at the LHC.

For this new jet algorithm, the parameter $\beta \geq 1$ specifies the algorithm and is introduced to determine the geometric size of the jet. By maximizing the $J_{E_T}^{(I)}$ function in Eq. (6), the final-state particles are forced into the collimated jets. For example, if the invariant mass m_J is large, the set will fail to produce a global maximum of $J_{E_T}^{(I)}$. This means only a subset that has large transverse energy but small invariant mass can form the jet. A reconstructed jet, thus, maximizes the function $J_{E_T}^{(I)}$ with the value

$$J_{E_T}^{(I)}(P^\mu_\mathrm{J}) \equiv E^\perp_\mathrm{J}\left[1 - \beta\frac{m^2_\mathrm{J}}{(E^\perp_\mathrm{J})^2}\right]. \quad (7)$$

In other words, when the jet is formed, the corresponding total four-momentum of the subset of the final-state particles P_set gives the jet momentum P_J, and $E^\perp_\mathrm{J}$ and m_J are the transverse energy and invariant mass of the jet, respectively. The algorithm is iterative; i.e., once a jet has been found, the algorithm proceeds by removing the subset from the list of particles in the event and applying iteratively to the remaining ones.

One may further vary the function $J_{E_T}^{(I)}$ by changing the weighted functions [38]. For instance, one can define the $J_{E_T}^{(n)}$ algorithm as follows:

$$J_{E_T}^{(n)}(P_{\rm J}^{\mu}) \equiv (E_{\rm set}^{\perp})^n \left[1 - \beta \frac{m_{\rm set}^2}{(E_{\rm set}^{\perp})^2}\right], \qquad (8)$$

where $n = 1$ and $n = 2$ correspond to the $J_{E_T}^{(I)}$ and $J_{E_T}^{(II)}$ algorithms,[1] respectively. In the present paper, we will focus on $J_{E_T}^{(I)}$ and $J_{E_T}^{(II)}$ algorithms to explicitly show the algorithm dependence of SIJFs. We will derive the NLO SIJFs by considering highly collimated jets, i.e., $\beta \gg 1$. In this case, one can take the so-called narrow jet approximation and obtain fully analytical expressions.

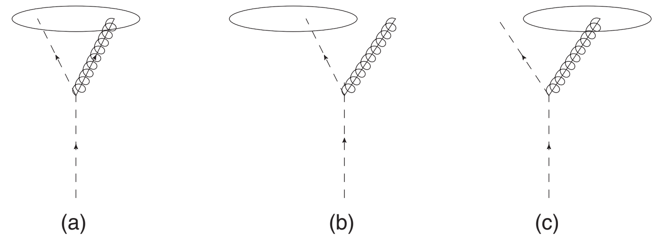

FIG. 1. The three situations that contribute to the semi-inclusive quark jet function: (A) both the quark and gluon are inside the jet, (B) only the quark is inside the jet, and (C) only the gluon is inside the jet.

III. THE SEMI-INCLUSIVE JET FUNCTIONS IN MAXIMIZED ALGORITHM

In this section, we present the detailed calculations at NLO for semi-inclusive jet functions for both quark and gluon jets in the maximized jet algorithm. As we have already mentioned, we perform the calculations in both light-cone gauge and covariant gauge for cross-checking our results, while the previous calculations are typically performed in covariant gauge; see, e.g., [25,49]. We denote the incoming parton with momentum $\ell = (\ell^- = \omega, \ell^+, 0_\perp)$ splits into two partons with one of them carry momentum $q = (q^-, q^+, q_\perp)$.

A. The semi-inclusive quark jet function

For the quark jet function, the total contributions from the relevant diagrams, as shown in Fig. 1, have been written down explicitly in $d = 4 - 2\epsilon$ dimensions in Ref. [25]. We rewrite it here for the completeness of showing the calculation:

$$J_q(z, E_{\rm J}) = g_s^2 \left(\frac{\mu^2 e^{\gamma_E}}{4\pi}\right)^{\epsilon} C_F \int \frac{d\ell^+}{2\pi} \frac{1}{\ell^+} \int \frac{d^d q}{(2\pi)^d} \left[4\frac{\ell^+}{q^-} + 2(1-\epsilon)\frac{\ell^+ - q^+}{\omega - q^-}\right] 2\pi\delta(q^+ q^- - q_\perp^2)$$
$$\times 2\pi\delta\left(\ell^+ - q^+ - \frac{q_\perp^2}{\omega - q^-}\right)\delta\left(z - \frac{\omega_{\rm J}}{\omega}\right)\Theta(q^-)\Theta(q^+)\Theta(\omega - q^-)\Theta(\ell^+ - q^+)\Theta_{\rm alg}. \qquad (9)$$

In this case, q denotes the momentum for the radiated gluon, and $\Theta_{\rm alg}$ is determined by the jet algorithm and by the kinematics of the radiated parton whether it is inside the jet. As shown in Fig. 1, there are three situations that we need to take into consideration. Diagram A is for the case that both quark and gluon are inside the jet, and diagrams B and C are for only the quark is inside the jet and only the gluon is inside the jet, respectively. Each case has different $\Theta_{\rm alg}$ to be specified below; the combination of these three cases gives the final result.

In the situation that both the quark and gluon are inside the jet, the incoming quark energy E is all converted to the jet energy $E_{\rm J}$, which leads to $z = E_{\rm J}/E = 1$. In this case, we can perform the integration over quantities ℓ^+ and q^+ in Eq. (9); thus, the quark jet function becomes

$$J_{q\to qg}(z, E_{\rm J}) = \delta(1-z)\frac{\alpha_s}{\pi}\frac{(\mu^2 e^{\gamma_E})^{\epsilon}}{\Gamma(1-\epsilon)}\int_0^1 dx \hat{P}_{qq}(x,\epsilon)[x(1-x)]^{-\epsilon}\int \frac{dm^2}{(m^2)^{1+\epsilon}}\Theta_{\rm alg}, \qquad (10)$$

where the subscript "$q \to qg$" stands for the situation that both the radiated quark and gluon are inside the jet, $x = (\ell^- - q^-)/\ell^-$ is the momentum fraction of the initial quark carried by the final-state quark, and $m^2 = \ell^2$ is the invariant mass for the final-state parton pair, i.e., $q + g$. Of course, since q and g together form the jet, $m^2 = m_{\rm J}^2$ is just the jet invariant mass, and it is related to the radiated gluon transverse momentum $q_\perp$ by $m^2 = \frac{q_\perp^2}{x(1-x)}$. The functions $\hat{P}_{ij}(x, \epsilon)$ are

$$\hat{P}_{qq}(x, \epsilon) = C_F\left[\frac{1+x^2}{1-x} - \epsilon(1-x)\right], \qquad (11)$$

[1]Technically speaking, the above $J_{E_T}^{(II)}$ corresponds only to a special (one-prong) case of the original definition given in Ref. [54]. This is sufficient for our purpose, where we focus on inclusive jet production and hadron distribution inside the jet and one-prong or two-prong distinction of the jet substructure is not needed.

$$\hat{P}_{gq}(x,\epsilon) = C_F\left[\frac{1+(1-x)^2}{x} - \epsilon x\right], \tag{12}$$

$$\hat{P}_{qg}(x,\epsilon) = T_F\left[1 - \frac{2x(1-x)}{1-\epsilon}\right], \tag{13}$$

$$\hat{P}_{gg}(x,\epsilon) = C_A\left[\frac{2x}{1-x} + \frac{2(1-x)}{x} + 2x(1-x)\right]. \tag{14}$$

In the channel $q \to qg$, to make sure that the final q and g actually form one jet, one has to require that the value of the $J_{E_T}^{(n)}$ function constructed from the two partons together is larger than the $J_{E_T}^{(n)}$ value constructed for each parton individually. When both q and g form the jet, we have

$$J_{E_T}^{(n)}(q+g) = E^n\left[1 - \beta\frac{m^2}{E^2}\right], \tag{15}$$

where we recall that E is the energy of the incoming quark and is the same as the jet energy $E_\mathrm{J} = E$ when q and g together form the jet. On the other hand, for the case in which either q or g forms the jet, we have

$$J_{E_T}^{(n)}(q) = (E_q)^n, \qquad J_{E_T}^{(n)}(g) = (E_g)^n, \tag{16}$$

where we have used the fact that the invariant mass of the final-state quark q or g vanishes. Thus, the requirements of the maximized jet algorithm $J_{E_T}^{(n)}(q+g) \geq J_{E_T}^{(n)}(q)$ and $J_{E_T}^{(n)}(q+g) \geq J_{E_T}^{(n)}(g)$ lead to the following constraint:

$$E^n\left[1 - \beta\frac{m^2}{E^2}\right] \geq \max\,[(E_q)^n, (E_g)^n]. \tag{17}$$

Realizing $E_q = xE$ and $E_g = (1-x)E$, we obtain the following constraint for m^2:

$$m^2 \leq \frac{E^2}{\beta}\min\,[1-(1-x)^n, 1-x^n]. \tag{18}$$

This leads to the following algorithm constraint:

$$\Theta_\mathrm{alg} = \Theta\left[\frac{E^2}{\beta}\min\,(1-(1-x)^n, 1-x^n) - m^2\right], \tag{19}$$

where Θ is the step function.

Let us first consider the $J_{E_T}^{(I)}$ algorithm; the calculation of the $J_{E_T}^{(II)}$ algorithm will follow the same procedure. Applying the above constraint to the jet function with $n=1$, we arrive at

$$J_{q\to qg}^{(I)}(z,E_\mathrm{J}) = \delta(1-z)\frac{\alpha_s}{2\pi}\frac{(\mu^2 e^{\gamma_E})^\epsilon}{\Gamma(1-\epsilon)}\left(-\frac{1}{\epsilon}\right)\left(\frac{E_\mathrm{J}^2}{\beta}\right)^{-\epsilon} I_{qq}^{(1)}, \tag{20}$$

where

$$I_{qq}^{(1)} \equiv \left[\int_0^{1/2} dx(1-(1-x))^{-\epsilon} + \int_{1/2}^1 dx(1-x)^{-\epsilon}\right] \times x^{-\epsilon}(1-x)^{-\epsilon}\hat{P}_{qq}(x). \tag{21}$$

Expanding $I_{qq}^{(1)}$ in ϵ, we get the explicit expression

$$I_{qq}^{(1)} = C_F\left[-\frac{1}{\epsilon} - \frac{3}{2} + \epsilon\left(-5 + \frac{\pi^2}{2} - \frac{3}{2}\ln 2\right)\right]. \tag{22}$$

Substituting the above expression to Eq. (20), we obtain the quark jet function when both the quark and gluon are inside the jet for the $J_{E_T}^{(I)}$ algorithm:

$$J_{q\to qg}^{(I)}(z,E_\mathrm{J}) = \delta(1-z)\frac{\alpha_s}{2\pi}C_F\left(\frac{1}{\epsilon^2} + \frac{3}{2\epsilon} + \frac{1}{\epsilon}\hat{L} + \frac{1}{2}\hat{L}^2 + \frac{3}{2}\hat{L} + 5 + \frac{3}{2}\ln 2 - \frac{7}{12}\pi^2\right), \tag{23}$$

with $\hat{L}$ defined as

$$\hat{L} = \ln\left(\frac{\beta\mu^2}{E_\mathrm{J}^2}\right). \tag{24}$$

For a highly collimated jet, i.e., $\beta \gg 1$, the above logarithmic term becomes very large and needs to be resummed. This is similar to that in k_t-type algorithms [25], where large logarithmic terms of R need to be resummed for small jet radius R.

Now let us consider the situation that only the final-state quark forms the jet. The corresponding diagram is presented in Fig. 1(b). In this case, the final-state quark forms the jet with jet energy $E_\mathrm{J} = zE$; namely, only a fraction z of the initial parton energy E falls inside the jet. Following the same calculation as before, we obtain

$$J_{q\to q(g)}(z,E_\mathrm{J}) = \frac{\alpha_s}{2\pi}\frac{(\mu^2 e^{\gamma_E})^\epsilon}{\Gamma(1-\epsilon)}\hat{P}_{qq}(z,\epsilon)[z(1-z)]^{-\epsilon}\int\frac{dm^2}{(m^2)^{1+\epsilon}}\Theta_\mathrm{alg}, \tag{25}$$

where the subscript $q \to q(g)$ represents the situation that only the quark q is inside the jet while the gluon g is radiated outside the jet. Here, m is again the invariant mass for the final-state parton pair, i.e., $q+g$. Since now only q is inside the jet while the gluon g is outside, m is different from the jet invariant mass.

In this case, it is the single quark that forms the jet, rather than the quark and gluon together forming a jet. Following the algorithm constraint, we should have

$$\max\,(J_{E_T}^{(n)}(q), J_{E_T}^{(n)}(g)) \geq J_{E_T}^{(n)}(q+g). \tag{26}$$

Note that this constraint is different from the original published version of Ref. [38], but the mistake has been corrected as an erratum to [38]. It turns out that only the constraint in Eq. (26) leads to the correct results for the SIJFs, which satisfy the momentum sum rule to be discussed at the end of Sec. III C. The above constraint can be understood as follows. If $J_{E_T}^{(n)}(g)$ is the larger one among $(J_{E_T}^{(n)}(q), J_{E_T}^{(n)}(g))$ and satisfies Eq. (26), then we would have a single gluon form the jet. Since the jet algorithm is iterative, the gluon jet will be removed from the event. As a result, we are left with only a single quark, which will automatically form another jet. On the contrary, if $J_{E_T}^{(n)}(q)$ is the larger one among $(J_{E_T}^{(n)}(q), J_{E_T}^{(n)}(g))$, the single quark first forms the jet. In other words, for a two-parton configuration, as long as the larger one among single-parton J_{E_T} functions is greater than the J_{E_T} function for the two-parton set, we will have the quark form the jet. With Eq. (26) at hand and from Eqs. (15) and (16), we thus have the following constraint:

$$\Theta_{\text{alg}} = \Theta\left[m^2 - \frac{E_{\text{J}}^2}{z^2\beta}\min\left[(1-z^n),(1-(1-z)^n)\right]\right], \tag{27}$$

where we have used $E = E_{\text{J}}/z$ for this configuration. Implementing this constraint in Eq. (25) and considering the case $n = 1$, we obtain

$$J_{q\to q(g)}^{(I)}(z,E_{\text{J}}) = \frac{\alpha_s}{2\pi}\frac{(\mu^2 e^{\gamma_E})^\epsilon}{\Gamma(1-\epsilon)}\left(\frac{1}{\epsilon}\right)\left(\frac{E_{\text{J}}^2}{\beta}\right)^{-\epsilon}\hat{P}_{qq}(z,\epsilon)[(1-z)^{-2\epsilon}z^\epsilon\Theta(z-1/2)+(1-z)^{-\epsilon}\Theta(1/2-z)]. \tag{28}$$

Performing the ϵ expansion, we find that the bare jet function is given as follows:

$$\begin{aligned} J_{q\to q(g)}^{(I)}(z,E_{\text{J}}) &= \frac{\alpha_s}{2\pi}C_F\delta(1-z)\left(-\frac{1}{\epsilon^2}-\frac{1}{\epsilon}L-\frac{1}{2}L^2+\frac{\pi^2}{12}\right) \\ &\quad + \frac{\alpha_s}{2\pi}C_F\left[\left(\frac{1}{\epsilon}+L\right)\frac{1+z^2}{(1-z)_+}-2(1+z^2)\left(\frac{\ln(1-z)}{1-z}\right)_+-(1-z)\right]+\frac{\alpha_s}{2\pi}C_F\frac{1+z^2}{1-z}\ln\left(\frac{1-z}{z}\right)\Theta(1/2-z), \end{aligned} \tag{29}$$

where

$$L = \hat{L} + \ln z = \ln\left(\frac{\beta\mu^2 z}{E_{\text{J}}^2}\right). \tag{30}$$

We realize that Eq. (29) is the same as that in the anti-k_T algorithm, except for the slightly different definition of L. The universality of this term is caused by the NJA, and the algorithm dependence is hidden in power-suppressed terms.

Likewise, for the case that only the gluon falls inside the jet, as illustrated in Fig. 1(c), the calculation is very similar to the case of $q \to q(g)$. For $n = 1$, it can be expressed as

$$J_{q\to(q)g}^{(I)}(z,E_{\text{J}}) = \frac{\alpha_s}{2\pi}\left(\frac{1}{\epsilon}+L\right)P_{gq}(z)-\frac{\alpha_s}{2\pi}C_F\left[\frac{1+(1-z)^2}{z}2\ln(1-z)+z\right]+\frac{\alpha_s}{2\pi}C_F\frac{1+(1-z)^2}{z}\ln\left(\frac{1-z}{z}\right)\Theta(1/2-z). \tag{31}$$

Summing Eqs. (23), (29), and (31) together, one obtains the full expression for the semi-inclusive quark jet function in the $J_{E_T}^{(I)}$ algorithm at NLO:

$$\begin{aligned} J_q^{(I)}(z,E_{\text{J}}) &= J_{q\to qg}^{(I)}(z,E_{\text{J}}) + J_{q\to q(g)}^{(I)}(z,E_{\text{J}}) + J_{q\to(q)g}^{(I)}(z,E_{\text{J}}) \\ &= \frac{\alpha_s}{2\pi}\left(\frac{1}{\epsilon}+L\right)[P_{qq}(z)+P_{gq}(z)]-\frac{\alpha_s}{2\pi}\left\{C_F\left[2(1+z^2)\left(\frac{\ln(1-z)}{1-z}\right)_+ +(1-z)\right]\right. \\ &\quad \left. -\delta(1-z)C_F\left(\frac{3\ln 2}{2}+5-\frac{\pi^2}{2}\right)+P_{gq}(z)2\ln(1-z)+C_F z-(P_{qq}(z)+P_{gq}(z))\ln\left(\frac{1-z}{z}\right)\Theta(1/2-z)\right\}, \end{aligned} \tag{32}$$

where $P_{ij}(z)$ are the standard Altarelli-Parisi splitting functions,

$$P_{qq}(z) = C_F\left[\frac{1+z^2}{(1-z)_+} + \frac{3}{2}\delta(1-z)\right], \tag{33}$$

$$P_{gq}(z) = C_F\frac{1+(1-z)^2}{z}, \tag{34}$$

$$P_{qg}(z) = T_F(z^2+(1-z)^2), \tag{35}$$

$$P_{gg}(z) = C_A\left[\frac{2z}{(1-z)_+} + \frac{2(1-z)}{z} + 2z(1-z)\right] + \frac{\beta_0}{2}\delta(1-z), \tag{36}$$

with $\beta_0 = \frac{11}{3}C_A - \frac{4}{3}T_F n_f$, and the "plus" distributions are defined as usual:

$$\int_0^1 dz f(z)[g(z)]_+ \equiv \int_0^1 dz[f(z)-f(1)]g(z). \tag{37}$$

Note that the double-pole term ($\propto 1/\epsilon^2$) as shown in $q\to qg$ channel cancel with that in $q\to q(g)$, and at the same time the $q\to(q)g$ channel is free of double-pole terms; thus, we are left with only a single-pole term (accordingly, single logarithm L) in the final result. The single-pole term is universal and independent of the jet algorithm, and it is this single-pole term that leads to the DGLAP evolution of the semi-inclusive jet functions [25].

Likewise, the jet function for the $J_{E_T}^{(II)}$ algorithm with $n=2$ can be derived by following exactly the same procedure as that for $n=1$. The final result is

$$\begin{aligned} J_q^{(II)}(z,E_{\rm J}) = {}& \frac{\alpha_s}{2\pi}\left(\frac{1}{\epsilon}+L\right)[P_{qq}(z)+P_{gq}(z)] - \frac{\alpha_s}{2\pi}\left\{C_F\left[2(1+z^2)\left(\frac{\ln(1-z)}{1-z}\right)_+ + (1-z)\right] + P_{gq}(z)2\ln(1-z) + C_F z\right. \\ & + [P_{qq}(z)+P_{gq}(z)]\left[\ln(1+z) + \ln\left(\frac{z(2-z)}{1-z^2}\right)\Theta(1/2-z)\right] \\ & \left. - \delta(1-z)C_F\left(-\frac{\pi^2}{2} + \frac{13}{2} - \frac{15\ln 2}{2} - \ln^2 2 + \frac{9\ln 3}{2} - \mathrm{Li}_2(1/4)\right)\right\}, \end{aligned} \tag{38}$$

where $\mathrm{Li}_2(1/4) = 0.267653\ldots$ is the dilogarithm function. We find that all the terms in the last two rows are algorithm dependent, while the rest of the terms are independent of the jet algorithm.

B. The semi-inclusive gluon jet function

The calculation of the semi-inclusive gluon jet function $J_g(z,E_{\rm J})$ is very similar to that for the quark jet case. As illustrated in Fig. 2, the semi-inclusive gluon jet function receives four contributions, including both $g\to gg$ and $g\to q\bar{q}$ splittings. For the case that both final-state partons are inside the jet, the semi-inclusive gluon jet function can be written as

$$J_{g\to gg+q\bar{q}}(z,E_{\rm J}) = \delta(1-z)\frac{\alpha_s}{2\pi}\frac{(\mu^2 e^{\gamma_E})^\epsilon}{\Gamma(1-\epsilon)}\int_0^1 dx\frac{1}{2}[2n_f\hat{P}_{qg}(x,\epsilon) + \hat{P}_{gg}(x,\epsilon)][x(1-x)]^{-\epsilon}\int\frac{dm^2}{(m^2)^{1+\epsilon}}\Theta_{\rm alg}, \tag{39}$$

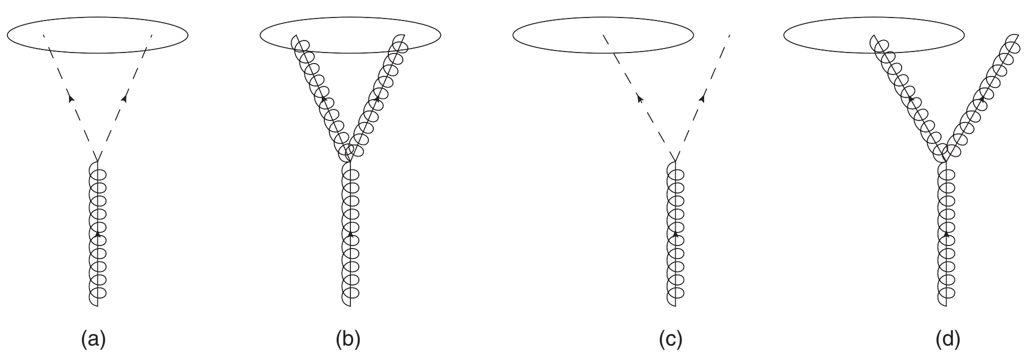

FIG. 2. The situations that contribute to the semi-inclusive gluon jet function when both final-state partons are inside the jet (A and B) and when only one of the final-state partons is inside the jet (C and D).

where n_f represents for the number of flavors of the final-state quark and $\hat{P}_{qg}(x,\epsilon)$ and $\hat{P}_{gg}(x,\epsilon)$ are given by Eqs. (13) and (14), respectively. In the situation when both the final-state partons are inside the jet, the constraint is shown in Eq. (19). Applying this constraint to Eq. (39), we obtain the semi-inclusive gluon jet function

$$J^{(I)}_{g\to gg+q\bar{q}}(z,E_\mathrm{J}) = \frac{\alpha_s}{2\pi}\frac{(\mu^2 e^{\gamma_E})^\epsilon}{\Gamma(1-\epsilon)}\left(-\frac{1}{\epsilon}\right)\left(\frac{E_\mathrm{J}^2}{\beta}\right)^{-\epsilon}\frac{1}{2}[2n_f I_{qg}+I_{gg}], \tag{40}$$

where

$$I_{ij} = \left[\int_0^{1/2}dx(1-(1-x))^{-\epsilon}+\int_{1/2}^1 dx(1-x)^{-\epsilon}\right]x^{-\epsilon} \times (1-x)^{-\epsilon}\hat{P}_{ij}(x,\epsilon). \tag{41}$$

Expanding to $\mathcal{O}(\epsilon)$, we obtain

$$I_{gg} = 2C_A\left[-\frac{1}{\epsilon}-\frac{11}{6}+\epsilon\left(-\frac{45}{8}+\frac{\pi^2}{2}-\frac{11}{6}\ln 2\right)\right], \tag{42}$$

$$I_{qg} = T_F\left[\frac{2}{3}+\epsilon\left(\frac{23}{12}+\frac{2}{3}\ln 2\right)\right]. \tag{43}$$

Inserting the above expressions into Eq. (40) and performing the ϵ expansion, we find

$$J^{(I)}_{g\to gg+q\bar{q}}(z,E_\mathrm{J}) = \delta(1-z)\frac{\alpha_s}{2\pi}\left[\frac{C_A}{\epsilon^2}+\frac{\beta_0}{2\epsilon}+\frac{C_A}{\epsilon}\hat{L}+\frac{C_A}{2}\hat{L}^2+\frac{\beta_0}{2}\hat{L}+C_A\left(\frac{45}{8}+\frac{11}{6}\ln 2-\frac{7\pi^2}{12}\right)-n_f T_F\left(\frac{23}{12}+\frac{2}{3}\ln 2\right)\right]. \tag{44}$$

We also need to consider the situation that only one of the partons forms the jet, and the corresponding Feynman diagrams are shown in Figs. 2(c) and 2(d). Summing these two diagrams together, we obtain

$$J_{g\to g(g)+q(\bar{q})}(z,E_\mathrm{J}) = \frac{\alpha_s}{2\pi}\frac{(\mu^2 e^{\gamma_E})^\epsilon}{\Gamma(1-\epsilon)}[\hat{P}_{gg}(z,\epsilon)+2n_f\hat{P}_{qg}(z,\epsilon)][z(1-z)]^{-\epsilon}\int\frac{dm^2}{(m^2)^{1+\epsilon}}\Theta_\mathrm{alg}. \tag{45}$$

With the constraint from the $J^{(I)}_{E_T}$ algorithm shown in Eq. (27), we can integrate over m^2 and then perform the ϵ expansion. The final results can be written as

$$\begin{aligned} J^{(I)}_{g\to g(g)+q(\bar{q})}(z,E_\mathrm{J},\mu) = {} & \frac{\alpha_s}{2\pi}\delta(1-z)\left(-\frac{C_A}{\epsilon^2}-\frac{\beta_0}{2\epsilon}-\frac{C_A}{\epsilon}L-\frac{C_A}{2}L^2-\frac{\beta_0}{2}L+\frac{\pi^2}{12}\right)+\frac{\alpha_s}{2\pi}\left(\frac{1}{\epsilon}+L\right)[P_{gg}(z)+2n_f P_{qg}(z)] \\ & -\frac{\alpha_s}{2\pi}\left\{\frac{4C_A(1-z+z^2)^2}{z}\left(\frac{\ln(1-z)}{1-z}\right)_+ + 4n_f[P_{qg}(z)\ln(1-z)+T_F z(1-z)] \right. \\ & \left. +[P_{gg}(z)+2n_f P_{qg}(z)]\ln\left(\frac{1-z}{z}\right)\Theta(1/2-z)\right\}. \end{aligned} \tag{46}$$

Finally, adding all contributions together, we obtain the following expression for the semi-inclusive gluon jet function:

$$\begin{aligned} J^{(I)}_g(z,E_\mathrm{J}) &= J^{(I)}_{g\to gg+q\bar{q}}(z,E_\mathrm{J})+J^{(I)}_{g\to g(g)+q(\bar{q})}(z,E_\mathrm{J}) \\ &= \frac{\alpha_s}{2\pi}\left(\frac{1}{\epsilon}+L\right)[P_{gg}(z)+2n_f P_{qg}(z)]-\frac{\alpha_s}{2\pi}\left\{\frac{4C_A(1-z+z^2)^2}{z}\left(\frac{\ln(1-z)}{1-z}\right)_+ + 4n_f[P_{qg}(z)\ln(1-z)\right. \\ &\quad + T_F z(1-z)] - \delta(1-z)\left[C_A\left(\frac{45}{8}+\frac{11}{6}\ln 2-\frac{\pi^2}{2}\right)-n_f T_F\left(\frac{23}{12}+\frac{2}{3}\ln 2\right)\right] \\ &\quad \left. -[P_{gg}(z)+2n_f P_{qg}(z)]\ln\left(\frac{1-z}{z}\right)\Theta(1/2-z)\right\}, \end{aligned} \tag{47}$$

where $P_{gg}(z)$ and $P_{qg}(z)$ are the standard Altarelli-Parisi splitting functions defined in Eqs. (35) and (36), respectively. Similar to the case for the quark jet, the double pole $1/\epsilon^2$ and the double logarithms L^2 cancel, and we are left with only a single pole $1/\epsilon$ and a single logarithm L.

Using the same procedure, we can also derive the semi-inclusive gluon jet function for the $J_{E_T}^{(II)}$ algorithm. The final expression is given by

$$J_g^{(II)}(z,E_\mathrm{J}) = \frac{\alpha_s}{2\pi}\left(\frac{1}{\epsilon}+L\right)[P_{gg}(z)+2n_fP_{qg}(z)] - \frac{\alpha_s}{2\pi}\left\{\frac{4C_A(1-z+z^2)^2}{z}\left(\frac{\ln(1-z)}{1-z}\right)_+ + 4n_f[P_{qg}(z)\ln(1-z)+T_Fz(1-z)] - \left[C_A\left(\frac{289}{36}-\frac{\pi^2}{2}-\frac{79\ln 2}{6}-\ln^2 2+\frac{15}{2}\ln 3-\mathrm{Li}_2(1/4)\right) - n_fT_f\left(\frac{67}{18}-\frac{34\ln 2}{3}+6\ln 3\right)\right]\times\delta(1-z)+[P_{gg}(z)+2n_fP_{qg}(z)] \times\left[\ln(1+z)+\ln\left(\frac{z(2-z)}{1-z^2}\right)\Theta(1/2-z)\right]\right\}, \tag{48}$$

where the last two rows in the above equation are algorithm dependent, while all the remaining terms are algorithm independent.

C. The RG evolution for semi-inclusive jet functions

The bare quark and gluon jet functions $J_{q,g}(z,E_\mathrm{J})$ are divergent, as they contain poles of $1/\epsilon$, which need to be renormalized. We follow the standard procedure and define the renormalized semi-inclusive jet functions $J_{q,g}(z,E_\mathrm{J},\mu)$ as follows:

$$J_i(z,E_\mathrm{J}) = \sum_j\int_z^1\frac{dz'}{z'}Z_{ij}\left(\frac{z}{z'},\mu\right)J_j(z',E_\mathrm{J},\mu), \tag{49}$$

where Z_{ij} is the renormalization matrix. Taking the derivative with respect to μ on both sides of the above equation, we can obtain the renormalization-group equation for the semi-inclusive jet function:

$$\mu\frac{d}{d\mu}J_i(z,E_\mathrm{J},\mu) = \sum_j\int_z^1\frac{dz'}{z'}\gamma_{ij}^J\left(\frac{z}{z'},\mu\right)J_j(z',E_\mathrm{J},\mu), \tag{50}$$

where γ_{ij}^J is the anomalous dimension related to the renormalization matrix

$$\gamma_{ij}^J(z,\mu) = -\sum_k\int_z^1\frac{dz'}{z'}(Z)^{-1}_{ik}\left(\frac{z}{z'},\mu\right)\mu\frac{d}{d\mu}Z_{kj}(z',\mu), \tag{51}$$

with the inverse of the renormalization factor $(Z)^{-1}_{ik}$ defined as

$$\sum_k\int_z^1\frac{dz'}{z'}(Z)^{-1}_{ik}\left(\frac{z}{z'},\mu\right)Z_{kj}(z',\mu) = \delta_{ij}\delta(1-z). \tag{52}$$

At LO, the renormalization matrix $Z_{ij}^{(0)}$ is purely δ function, which is given by $Z_{ij}^{(0)}(z,\mu) = \delta_{ij}\delta(1-z)$. At NLO, the one-loop renormalization factors $Z_{ij}^{(1)}$ can be extracted from the pole terms in the final result of the bare semi-inclusive jet function shown in Eqs. (47) and (48):

$$Z_{ij}^{(1)}(z,\mu) = \frac{\alpha_s(\mu)}{2\pi}\left(\frac{1}{\epsilon}\right)P_{ji}(z), \tag{53}$$

from which we obtain the anomalous dimension

$$\gamma_{ij}^J = \frac{\alpha_s(\mu)}{\pi}P_{ji}(z). \tag{54}$$

Thus, the renormalization-group equations for the renormalized SIJFs is just the timelike DGLAP evolution equation for the usual fragmentation functions

$$\mu\frac{d}{d\mu}J_i(z,E_\mathrm{J},\mu) = \frac{\alpha_s(\mu)}{\pi}\sum_j\int_z^1\frac{dz'}{z'}P_{ji}\left(\frac{z}{z'}\right)J_j(z',E_\mathrm{J},\mu). \tag{55}$$

The divergence of $Z_{ij}^{(1)}$ cancels exactly with the divergence in the bare semi-inclusive jet functions and eventually leads to finite renormalized semi-inclusive jet functions. For the maximized algorithm with $n=1$, i.e., $J_{E_T}^{(I)}$, we have the following expressions for the renormalized SIJFs at NLO:

$$J_q^{(I)}(z,E_\mathrm{J},\mu)=\delta(1-z)+\frac{\alpha_s}{2\pi}L[P_{qq}(z)+P_{gq}(z)]-\frac{\alpha_s}{2\pi}\left\{C_F\left[2(1+z^2)\left(\frac{\ln(1-z)}{1-z}\right)_+ +(1-z)\right]\right.$$
$$\left.-\delta(1-z)C_F\left(\frac{3\ln 2}{2}+5-\frac{\pi^2}{2}\right)+P_{gq}(z)2\ln(1-z)+C_Fz-(P_{qq}(z)+P_{gq}(z))\ln\left(\frac{1-z}{z}\right)\Theta(1/2-z)\right\}, \tag{56}$$

$$J_g^{(I)}(z,E_\mathrm{J},\mu)=\delta(1-z)+\frac{\alpha_s}{2\pi}L[P_{gg}(z)+2n_fP_{qg}(z)]-\frac{\alpha_s}{2\pi}\left\{\frac{4C_A(1-z+z^2)^2}{z}\left(\frac{\ln(1-z)}{1-z}\right)_+\right.$$
$$+4n_f[P_{qg}(z)\ln(1-z)+T_Fz(1-z)]-\delta(1-z)\left[C_A\left(\frac{45}{8}+\frac{11}{6}\ln 2-\frac{\pi^2}{2}\right)-n_fT_F\left(\frac{23}{12}+\frac{2}{3}\ln 2\right)\right]$$
$$\left.-[P_{gg}(z)+2n_fP_{qg}(z)]\ln\left(\frac{1-z}{z}\right)\Theta(1/2-z)\right\}. \tag{57}$$

On the other hand, for the maximized algorithm with $n=2$, i.e., $J_{E_T}^{(II)}$, the SIJFs at NLO can be written as follows:

$$J_q^{(II)}(z,E_\mathrm{J},\mu)=\delta(1-z)+\frac{\alpha_s}{2\pi}L[P_{qq}(z)+P_{gq}(z)]-\frac{\alpha_s}{2\pi}\left\{C_F\left[2(1+z^2)\left(\frac{\ln(1-z)}{1-z}\right)_+ +(1-z)\right]\right.$$
$$+P_{gq}(z)2\ln(1-z)+C_Fz+[P_{qq}(z)+P_{gq}(z)]\left[\ln(1+z)+\ln\left(\frac{z(2-z)}{1-z^2}\right)\Theta(1/2-z)\right]$$
$$\left.-\delta(1-z)C_F\left(-\frac{\pi^2}{2}+\frac{13}{2}-\frac{15\ln 2}{2}-\ln^2 2+\frac{9\ln 3}{2}-\mathrm{Li}_2(1/4)\right)\right\}, \tag{58}$$

$$J_g^{(II)}(z,E_\mathrm{J},\mu)=\delta(1-z)+\frac{\alpha_s}{2\pi}L[P_{gg}(z)+2n_fP_{qg}(z)]$$
$$-\frac{\alpha_s}{2\pi}\left\{\frac{4C_A(1-z+z^2)^2}{z}\left(\frac{\ln(1-z)}{1-z}\right)_+ +4n_f[P_{qg}(z)\ln(1-z)+T_Fz(1-z)]\right.$$
$$-\left[C_A\left(\frac{289}{36}-\frac{\pi^2}{2}-\frac{79\ln 2}{6}-\ln^2 2+\frac{15}{2}\ln 3-\mathrm{Li}_2(1/4)\right)-n_fT_f\left(\frac{67}{18}-\frac{34\ln 2}{3}+6\ln 3\right)\right]\times\delta(1-z)$$
$$\left.+[P_{gg}(z)+2n_fP_{qg}(z)]\left[\ln(1+z)+\ln\left(\frac{z(2-z)}{1-z^2}\right)\Theta(1/2-z)\right]\right\}. \tag{59}$$

It is important to point out that the natural scale μ_J for the SIJFs can be derived from Eq. (30):

$$\mu_\mathrm{J}^2=\frac{E_\mathrm{J}^2}{\beta z}. \tag{60}$$

Thus, by solving the DGLAP evolution equation (55) and, thus, evolving the SIJFs from its natural scale μ_J to the hard scattering scale $\mu\sim E_\mathrm{J}$, we can resum large logarithms of the jet size parameter β. This is similar to the small jet radius $\ln R$ resummation developed in Ref. [25]. It might be worthwhile to point out that the momentum fraction z also plays some role in this evolution, and it would be valuable to study numerically how important such an effect is. Finally, it is interesting to point out that the above renormalized semi-inclusive jet functions satisfy the following momentum sum rule [26,53]:

$$\int_0^1 dzzJ_i(z,E_\mathrm{J}=zE,\mu)=1. \tag{61}$$

This momentum conservation rule provides us an alternative way to check our results. It is instructive to point out that the correct jet algorithm constraint in Eq. (26) for the situation where a single parton forms the jet is crucial to derive the correct SIJFs. Otherwise, the obtained results for the SIJFs will not satisfy the momentum sum rule. In this context, the momentum sum rule derived from the operator definition of the SIJFs in SCET can play an important role. Thus, performing the calculations directly from the operator definitions for the SIJFs as we have done in this section shows some advantages.

Note that the above semi-inclusive jet functions were first derived in Refs. [27,38] via standard pQCD techniques. Our results are slightly different from those in the originally published version of Refs. [27,38]. However, those results are now corrected and updated as an erratum to [27,38]. Our results are consistent with those in the updated version.

IV. THE SEMI-INCLUSIVE FRAGMENTING JET FUNCTIONS

We now turn to the evaluation of jet substructure with maximized jet algorithms. In this section, we focus on the so-called SIFJFs as initially introduced in Ref. [28]. The SIFJFs describe the longitudinal momentum distribution of hadrons inside the jet. Comparing to the SIJFs, we need one more variable, $\omega_h \approx 2E_h$, to represent for the light-cone momentum of the observed hadron. Accordingly, $z_h = E_h/E_\mathrm{J}$ denotes the fraction of the jet energy carried by the observed hadron. In this section, we will first introduce the definition of SIFJFs in SCET, and we then present their NLO calculations for both the $J_{E_T}^{(I)}$ and $J_{E_T}^{(II)}$ algorithms. We will present the detailed steps of our calculations for the $J_{E_T}^{(I)}$ algorithm. At the end of the section, we will write down the results for the $J_{E_T}^{(II)}$ algorithm, as the procedure is very similar.

Similar to the SIJFs, one can define the SIFJFs for quark and gluon jets in terms of gauge-invariant quark and gluon fields in SCET [28]:

$$\mathcal{G}_q^h(z, z_h, E_\mathrm{J}) = \frac{z}{2N_c}\delta\left(z_h - \frac{E_h}{E_\mathrm{J}}\right)\mathrm{Tr}\left[\frac{\bar{\not n}}{2}\langle 0|\delta(\omega - \bar{n}\cdot\mathcal{P})\chi_n(0)|(Jh)X\rangle\langle(Jh)X|\bar{\chi}_n(0)|0\rangle\right],$$
$$\mathcal{G}_g^h(z, z_h, E_\mathrm{J}) = -\frac{z\omega}{(d-2)(N_c^2-1)}\delta\left(z_h - \frac{E_h}{E_\mathrm{J}}\right)\langle 0|\delta(\omega - \bar{n}\cdot\mathcal{P})\mathcal{B}_{n\perp\mu}(0)|(Jh)X\rangle\langle(Jh)X|\mathcal{B}_{n\perp}^{\mu}(0)|0\rangle, \tag{62}$$

where $(d-2)$ is the number of polarizations for initial gluons in d dimension. The state $|(Jh)X\rangle$ represents the final-state identified hadron (h) inside the jet J as denoted by (Jh), and X stands for unobserved particles. On the other hand, ω, E_J, and z have exactly the same meaning as those in SIJFs.

Different from the semi-inclusive jet functions as discussed in the previous section, the SIFJFs involve the hadronic scale, thus contain nonperturbative information, and are, in principle, not calculable in pQCD. However, the matching coefficients between SIFJFs and standard fragmentation functions can be determined perturbatively; thus, one can simply replace the hadronic states in Eq. (62) by the corresponding partonic states, which allows us to use the methodology of pQCD. In the following, we will show explicitly the calculation of $\mathcal{G}_i^j$ with i the initial parton and j the fragmenting parton. Similar to SIJFs, the SIFJFs at LO involve only delta functions:

$$\mathcal{G}_i^{j,(0)}(z, z_h, E_\mathrm{J}) = \delta_{ij}\delta(1-z)\delta(1-z_h). \tag{63}$$

The last two delta functions correspond to the case that the total energy of the initiating parton is transferred to the jet, and the fragmenting parton carries the whole energy of the jet.

A. Fragmenting jet functions at NLO

At NLO, the initiating parton splits into two partons, which leads to two contributions for SIFJFs: One is for the case when both partons are inside the jet, and another case is when only one parton is inside the jet. In the situation that both partons are inside the jet, the corresponding Feynman diagrams for quark- and gluon-initiated jet are shown in Figs. 1(a) and 2(a), respectively. In this case, all the initial parton energy E stays inside the jet; thus, $z = E_\mathrm{J}/E = 1$. Different with the semi-inclusive jet functions, we now observe a particular fragmenting parton inside the jet, where the fragmenting parton carries only part of the jet energy as characterized by $z_h = E_h/E_\mathrm{J} < 1$. In the $\overline{\mathrm{MS}}$ scheme, the one-loop bare SIFJFs can be written as [28]

$$\mathcal{G}_{i,\mathrm{bare}}^{jk,(1)}(z, z_h, E_\mathrm{J}) = \delta(1-z)\frac{\alpha_s}{2\pi}\frac{(e^{\gamma_E}\mu^2)^\epsilon}{\Gamma(1-\epsilon)}\int_0^1 dx\,\delta(x - z_h) \times \hat{P}_{ji}(x,\epsilon)[x(1-x)]^{-\epsilon}\int\frac{dm^2}{(m^2)^{1+\epsilon}}\Theta_\mathrm{alg}. \tag{64}$$

In comparison with the SIJFs in Eq. (10), the above expression is different only by a factor $\delta(x - z_h)$, since we now measure the momentum fraction carried by the final-state parton. Similar to that in semi-inclusive jet functions, "jk" indicates the situation that both split partons j and k remain inside the jet. The functions $\hat{P}_{ji}(x,\epsilon)$ are given by Eqs. (11)–(14).

To proceed with the NLO calculation, we implement the jet algorithm constraint, given already in Eq. (19), at the same time integrate x with the help of the $\delta(x - z_h)$ function in Eq. (64), and can derive the final result. It turns out that the result depends on the value of z_h. When $z_h \leq 1/2$, we have

$$\int \frac{dm^2}{(m^2)^{1+\epsilon}}\Theta_{\text{alg}} = \int_0^{(E_J^2/\beta)(1-(1-z_h))} = \left(-\frac{1}{\epsilon}\right)\left(\frac{E_J^2}{\beta}\right)^{-\epsilon}(1-(1-z_h))^{-\epsilon}. \tag{65}$$

For $z_h \geq 1/2$, we have the following expression:

$$\int \frac{dm^2}{(m^2)^{1+\epsilon}}\Theta_{\text{alg}} = \int_0^{(E_J^2/\beta)(1-z_h)} = \left(-\frac{1}{\epsilon}\right)\left(\frac{E_J^2}{\beta}\right)^{-\epsilon}(1-z_h)^{-\epsilon}. \tag{66}$$

Substituting these two integrals into Eq. (64), we obtain the following result for the case when both partons are inside the jet:

$$\begin{aligned}\mathcal{G}_{i,\text{bare}}^{jk,(1)}(z,z_h,E_J) = \delta(1-z)\frac{\alpha_s}{2\pi}\frac{(e^{\gamma_E}\mu^2)^\epsilon}{\Gamma(1-\epsilon)}\hat{P}_{ji}(z_h,\epsilon)\left(-\frac{1}{\epsilon}\right)\left(\frac{E_J^2}{\beta}\right)^{-\epsilon}\left[(z_h)^{-2\epsilon}(1-z_h)^{-\epsilon}\theta\left(\frac{1}{2}-z_h\right)\right.\\ \left. + (z_h)^{-\epsilon}(1-z_h)^{-2\epsilon}\theta\left(z_h-\frac{1}{2}\right)\right].\end{aligned} \tag{67}$$

Now we turn to the case that only one parton is inside the jet. The corresponding diagrams are shown in Figs. 1(b) and 1(c) for the quark-initiated jet and Figs. 2(c) and 2(d) for the gluon-initiated jet. In this case, the final-state fragmenting parton forms the jet; thus, we have $z < 1$. On the other hand, within the jet, there is only one parton at NLO which is eventually converted to the fragmenting parton. This leads to an overall delta function ensuring $z_h = 1$; i.e., all the jet energy is translated into the fragmenting parton energy. Performing the evaluation of diagrams in Figs. 1(b), 1(c), 2(c), and 2(d), we obtain the bare SIFJFs when only parton j forms the jet:

$$\mathcal{G}_{i,\text{bare}}^{j(k),(1)}(z,z_h,E_J) = \delta(1-z_h)\frac{\alpha_s}{2\pi}\frac{(e^{\gamma_E}\mu^2)^\epsilon}{\Gamma(1-\epsilon)}\hat{P}_{ji}(z,\epsilon)z^{-\epsilon}(1-z)^{-\epsilon}\int\frac{dm^2}{(m^2)^{1+\epsilon}}\Theta_{\text{alg}}, \tag{68}$$

where the superscript $j(k)$ indicates that parton j is inside the jet while k exits the jet. We can now implement the jet algorithm constraint Eq. (27) in the m^2 integration, and we obtain for the $J_{E_T}^{(I)}$ algorithm

$$\int \frac{dm^2}{(m^2)^{1+\epsilon}}\Theta_{\text{alg}} = \int_{(E_J^2/z^2\beta)\ \min[1-z,z]}^{\infty}\frac{dm^2}{(m^2)^{1+\epsilon}} = \left(\frac{1}{\epsilon}\right)\left(\frac{E_J^2}{\beta}\right)^{-\epsilon}[(1-z)^{-\epsilon}z^{2\epsilon}\Theta(z-1/2)+z^\epsilon\Theta(1/2-z)]. \tag{69}$$

With the above result at hand, we can write the second contribution of the bare SIFJFs as follows:

$$\mathcal{G}_{i,\text{bare}}^{j(k),(1)}(z,z_h,E_J) = \delta(1-z_h)\frac{\alpha_s}{2\pi}\frac{(e^{\gamma_E}\mu^2)^\epsilon}{\Gamma(1-\epsilon)}\hat{P}_{ji}(z,\epsilon)\left(\frac{1}{\epsilon}\right)\left(\frac{E_J^2}{\beta}\right)^{-\epsilon}[(1-z)^{-2\epsilon}z^\epsilon\Theta(z-1/2)+(1-z)^{-\epsilon}\Theta(1/2-z)]. \tag{70}$$

Summing the two contributions shown in Eqs. (67) and (70), we obtain the following results for the bare SIFJFs at NLO:

$$\begin{aligned}\mathcal{G}_{i,\text{bare}}^{j}(z,z_h,E_J) &= \mathcal{G}_{i,\text{bare}}^{j,(0)}(z,z_h,E_J,\mu) + \mathcal{G}_{i,\text{bare}}^{jk,(1)}(z,z_h,E_J) + \mathcal{G}_{i,\text{bare}}^{j(k),(1)}(z,z_h,E_J)\\ &= \delta_{ij}\delta(1-z)\delta(1-z_h) + \frac{\alpha_s}{2\pi}\frac{(e^{\gamma_E}\mu^2)^\epsilon}{\Gamma(1-\epsilon)}\left(-\frac{1}{\epsilon}\right)\left(\frac{E_J^2}{\beta}\right)^{-\epsilon}\\ &\quad\times\{\delta(1-z)\hat{P}_{ji}(z_h,\epsilon)[(z_h)^{-2\epsilon}(1-z_h)^{-\epsilon}\Theta(1/2-z_h)+(z_h)^{-\epsilon}(1-z_h)^{-2\epsilon}\Theta(z_h-1/2)]\\ &\quad-\delta(1-z_h)\hat{P}_{ji}(z,\epsilon)[(1-z)^{-2\epsilon}z^\epsilon\Theta(z-1/2)+(1-z)^{-\epsilon}\Theta(1/2-z)]\}.\end{aligned} \tag{71}$$

Performing ϵ expansion, we obtain the explicit expression of the SIFJFs for the $J_{E_T}^{(I)}$ algorithm:

$$
\begin{aligned}
\mathcal{G}_{q,\mathrm{bare}}^{q,(I)}(z,z_h,E_\mathrm{J}) = {}& \delta(1-z)\delta(1-z_h) + \frac{\alpha_s}{2\pi}\left(-\frac{1}{\epsilon}-L\right)P_{qq}(z_h)\delta(1-z) + \frac{\alpha_s}{2\pi}\left(\frac{1}{\epsilon}+L\right)P_{qq}(z)\delta(1-z_h) \\
&+ \delta(1-z)\frac{\alpha_s}{2\pi}\left[2C_F(1+z_h^2)\left(\frac{\ln(1-z_h)}{1-z_h}\right)_+ + C_F(1-z_h)\right] \\
&+ \delta(1-z)\frac{\alpha_s}{2\pi}\left[P_{qq}(z_h)\ln z_h + \Theta(1/2-z_h)P_{qq}(z_h)\ln\left(\frac{z_h}{1-z_h}\right)\right] \\
&- \delta(1-z_h)\frac{\alpha_s}{2\pi}\left[2C_F(1+z^2)\left(\frac{\ln(1-z)}{1-z}\right)_+ + C_F(1-z) - P_{qq}(z)\ln\left(\frac{1-z}{z}\right)\Theta(1/2-z)\right], \qquad (72)
\end{aligned}
$$

$$
\begin{aligned}
\mathcal{G}_{g,\mathrm{bare}}^{g,(I)}(z,z_h,E_\mathrm{J}) = {}& \delta(1-z)\delta(1-z_h) + \frac{\alpha_s}{2\pi}\left(-\frac{1}{\epsilon}-L\right)P_{gg}(z_h)\delta(1-z) + \frac{\alpha_s}{2\pi}\left(\frac{1}{\epsilon}+L\right)P_{gg}(z)\delta(1-z_h) \\
&+ \delta(1-z)\frac{\alpha_s}{2\pi}\left[4C_A\frac{(1-z_h+z_h^2)^2}{z_h}\left(\frac{\ln(1-z_h)}{1-z_h}\right)_+\right] \\
&+ \delta(1-z)\frac{\alpha_s}{2\pi}\left[P_{gg}(z_h)\ln z_h + \Theta(1/2-z_h)P_{gg}(z_h)\ln\left(\frac{z_h}{1-z_h}\right)\right] \\
&- \delta(1-z_h)\frac{\alpha_s}{2\pi}\left[4C_A\frac{(1-z+z^2)^2}{z}\left(\frac{\ln(1-z)}{1-z}\right)_+ - P_{gg}(z)\ln\left(\frac{1-z}{z}\right)\Theta(1/2-z)\right], \qquad (73)
\end{aligned}
$$

$$
\begin{aligned}
\mathcal{G}_{q,\mathrm{bare}}^{g,(I)}(z,z_h,E_\mathrm{J}) = {}& \frac{\alpha_s}{2\pi}\left(-\frac{1}{\epsilon}-L\right)P_{gq}(z_h)\delta(1-z) + \frac{\alpha_s}{2\pi}\left(\frac{1}{\epsilon}+L\right)P_{gq}(z)\delta(1-z_h) \\
&+ \delta(1-z)\frac{\alpha_s}{2\pi}[2P_{gq}(z_h)\ln(1-z_h) + C_F z_h] \\
&+ \delta(1-z)\frac{\alpha_s}{2\pi}\left[P_{gq}(z_h)\ln z_h + \Theta(1/2-z_h)P_{gq}(z_h)\ln\left(\frac{z_h}{1-z_h}\right)\right] \\
&- \delta(1-z_h)\frac{\alpha_s}{2\pi}\left[2P_{gq}(z)\ln(1-z) + C_F z - P_{gq}(z)\ln\left(\frac{1-z}{z}\right)\Theta(1/2-z)\right], \qquad (74)
\end{aligned}
$$

$$
\begin{aligned}
\mathcal{G}_{g,\mathrm{bare}}^{q,(I)}(z,z_h,E_\mathrm{J}) = {}& \frac{\alpha_s}{2\pi}\left(-\frac{1}{\epsilon}-L\right)P_{qg}(z_h)\delta(1-z) + \frac{\alpha_s}{2\pi}\left(\frac{1}{\epsilon}+L\right)P_{qg}(z)\delta(1-z_h) \\
&+ \delta(1-z)\frac{\alpha_s}{2\pi}[2P_{qg}(z_h)\ln(1-z_h) + 2T_F z_h(1-z_h)] \\
&+ \delta(1-z)\frac{\alpha_s}{2\pi}\left[P_{qg}(z_h)\ln z_h + \Theta(1/2-z_h)P_{qg}(z_h)\ln\left(\frac{z_h}{1-z_h}\right)\right] \\
&- \delta(1-z_h)\frac{\alpha_s}{2\pi}\left[2P_{qg}(z)\ln(1-z) + 2T_F z(1-z) - P_{qg}(z)\ln\left(\frac{1-z}{z}\right)\Theta(1/2-z)\right], \qquad (75)
\end{aligned}
$$

where the logarithm L is defined in Eq. (30) and the Altarelli-Parisi splitting functions are defined in Eqs. (33)–(36).

The results for the bare SIFJFs at NLO for the $J_{E_T}^{(II)}$ algorithm can be obtained similarly, and they are given by

$$\begin{aligned}\mathcal{G}_{q,\mathrm{bare}}^{q,(II)}(z,z_h,E_\mathrm{J}) &= \delta(1-z)\delta(1-z_h) + \frac{\alpha_s}{2\pi}\left(-\frac{1}{\epsilon}-L\right)P_{qq}(z_h)\delta(1-z) + \frac{\alpha_s}{2\pi}\left(\frac{1}{\epsilon}+L\right)P_{qq}(z)\delta(1-z_h)\\ &+\delta(1-z)\frac{\alpha_s}{2\pi}\left[2C_F(1+z_h^2)\left(\frac{\ln(1-z_h)}{1-z_h}\right)_+ + C_F(1-z_h)\right]\\ &+\delta(1-z)\frac{\alpha_s}{2\pi}\left[\tilde{P}_{qq}(z_h)\ln(z_h(1+z_h)) + \Theta(1/2-z_h)P_{qq}(z_h)\ln\left(\frac{z_h(2-z_h)}{1-z_h^2}\right)\right]\\ &-\delta(1-z_h)\frac{\alpha_s}{2\pi}\left[2C_F(1+z^2)\left(\frac{\ln(1-z)}{1-z}\right)_+ + C_F(1+z^2)\frac{\ln(1+z)}{(1-z)_+} + C_F(1-z)\right.\\ &\left.+P_{qq}(z)\ln\left(\frac{z(2-z)}{1-z^2}\right)\Theta(1/2-z)\right],\end{aligned} \tag{76}$$

$$\begin{aligned}\mathcal{G}_{g,\mathrm{bare}}^{g,(II)}(z,z_h,E_\mathrm{J}) &= \delta(1-z)\delta(1-z_h) + \frac{\alpha_s}{2\pi}\left(-\frac{1}{\epsilon}-L\right)P_{gg}(z_h)\delta(1-z) + \frac{\alpha_s}{2\pi}\left(\frac{1}{\epsilon}+L\right)P_{gg}(z)\delta(1-z_h)\\ &+\delta(1-z)\frac{\alpha_s}{2\pi}\left[4C_A\frac{(1-z_h+z_h^2)^2}{z_h}\left(\frac{\ln(1-z_h)}{1-z_h}\right)_+\right]\\ &+\delta(1-z)\frac{\alpha_s}{2\pi}\left[\tilde{P}_{gg}(z_h)\ln(z_h(1+z_h)) + \Theta(1/2-z_h)P_{gg}(z_h)\ln\left(\frac{z_h(2-z_h)}{1-z_h^2}\right)\right]\\ &-\delta(1-z_h)\frac{\alpha_s}{2\pi}\left[4C_A\frac{(1-z+z^2)^2}{z}\left(\frac{\ln(1-z)}{1-z}\right)_+ + 2C_A\frac{(1-z+z^2)^2}{z}\frac{\ln(1+z)}{(1-z)_+}\right.\\ &\left.+P_{gg}(z)\ln\left(\frac{z(2-z)}{1-z^2}\right)\Theta(1/2-z)\right],\end{aligned} \tag{77}$$

$$\begin{aligned}\mathcal{G}_{q,\mathrm{bare}}^{g,(II)}(z,z_h,E_\mathrm{J}) &= \frac{\alpha_s}{2\pi}\left(-\frac{1}{\epsilon}-L\right)P_{gq}(z_h)\delta(1-z) + \frac{\alpha_s}{2\pi}\left(\frac{1}{\epsilon}+L\right)P_{gq}(z)\delta(1-z_h)\\ &+\delta(1-z)\frac{\alpha_s}{2\pi}[2P_{gq}(z_h)\ln(1-z_h) + C_F z_h]\\ &+\delta(1-z)\frac{\alpha_s}{2\pi}\left[P_{gq}(z_h)\ln(z_h(1+z_h)) + \Theta(1/2-z_h)P_{gq}(z_h)\ln\left(\frac{z_h(2-z_h)}{1-z_h^2}\right)\right]\\ &-\delta(1-z_h)\frac{\alpha_s}{2\pi}\left[2P_{gq}(z)\ln(1-z) + P_{gq}(z)\ln(1+z) + C_F z + P_{gq}(z)\ln\left(\frac{z(2-z)}{1-z^2}\right)\Theta(1/2-z)\right],\end{aligned} \tag{78}$$

$$\begin{aligned}\mathcal{G}_{g,\mathrm{bare}}^{q,(II)}(z,z_h,E_\mathrm{J}) &= \frac{\alpha_s}{2\pi}\left(-\frac{1}{\epsilon}-L\right)P_{qg}(z_h)\delta(1-z) + \frac{\alpha_s}{2\pi}\left(\frac{1}{\epsilon}+L\right)P_{qg}(z)\delta(1-z_h)\\ &+\delta(1-z)\frac{\alpha_s}{2\pi}[2P_{qg}(z_h)\ln(1-z_h) + 2T_F z_h(1-z_h)]\\ &+\delta(1-z)\frac{\alpha_s}{2\pi}\left[P_{qg}(z_h)\ln(z_h(1+z_h)) + \Theta(1/2-z_h)P_{qg}(z_h)\ln\left(\frac{z_h(2-z_h)}{1-z_h^2}\right)\right]\\ &-\delta(1-z_h)\frac{\alpha_s}{2\pi}\left[2P_{qg}(z)\ln(1-z) + P_{qg}(z)\ln(1+z) + 2T_F z(1-z)\right.\\ &\left.+P_{qg}(z)\ln\left(\frac{z(2-z)}{1-z^2}\right)\Theta(1/2-z)\right],\end{aligned} \tag{79}$$

where $\tilde{P}_{qq}(z)$ and $\tilde{P}_{gg}(z)$ are the Altarelli-Parisi splitting functions defined in Eqs. (33) and (36), but with the $\delta(1-z)$ term removed. For later convenience, we also define $\tilde{P}_{gq}(z) = P_{gq}(z)$ and $\tilde{P}_{qg}(z) = P_{qg}(z)$. Notice that the pole terms are universal for different jet algorithms. This is why all these semi-inclusive jet functions follow the same timelike DGLAP evolution equations [28].

B. Renormalization and matching

From the final expressions of the bare SIFJFs $\mathcal{G}_i^j(z, z_h, E_J)$, single-pole terms still remain, which include both infrared (IR) poles as identified in association with $P_{ji}(z_h)\delta(1-z)$ and the ultraviolet (UV) poles that multiplied by $P_{ji}(z)\delta(1-z_h)$. The standard procedure to subtract the UV poles is realized by the definition of renormalized SIFJFs. After the renormalization, we find the following renormalization group equations for the renormalized SIFJFs $\mathcal{G}_i^h(z, z_h, E_J, \mu)$:

$$\mu\frac{d}{d\mu}\mathcal{G}_i^h(z, z_h, E_J, \mu) = \frac{\alpha_s(\mu)}{\pi}\sum_j \int_z^1 \frac{dz'}{z'} P_{ji}\left(\frac{z}{z'}\right)\mathcal{G}_k^j(z', z_h, E_J, \mu), \quad (80)$$

which is the same as the usual timelike DGLAP evolution equation, just like that for the SIJFs in Eq. (55). From the perturbative calculations of $\mathcal{G}_i^h(z, z_h, E_J, \mu)$, we find that the natural scale for the SIFJFs is again $\mu_{\mathcal{G}}^2 \sim E_J^2/\beta z$. Thus, solving the above evolution equations and evolving the SIFJFs from $\mu_{\mathcal{G}}$ to the typical hard scale $\mu \sim E_J$, one again achieves the resummation of $\ln\beta$. This could be very important for highly collimated jets where $\beta \gg 1$.

It is important to emphasize that the renormalization equations for SIFJFs are universal and independent of specific jet algorithms. Different to the SIJFs shown in Sec. III, there is explicit flavor dependence for SIFJFs due to the involved fragmentation functions. This leads to more complicated flavor separation in solving the renormalization equations for SIFJFs than that for SIJFs. For details, see Ref. [28]. After renormalization, the remaining IR poles are removed by matching the renormalized SIFJFs $\mathcal{G}_i^j(z, z_h, E_J, \mu)$ onto the fragmentation functions $D_i^h(z_h, \mu)$ at a scale $\mu \gg \Lambda_{\mathrm{QCD}}$ as follows:

$$\mathcal{G}_i^h(z, z_h, E_J, \mu) = \sum_j \int_{z_h}^1 \frac{dz_h'}{z_h'}\mathcal{J}_{ij}(z, z_h', E_J, \mu) D_j^h\left(\frac{z_h}{z_h'}, \mu\right). \quad (81)$$

To derive the matching coefficients $\mathcal{J}_{ij}$, we again replace the hadron h by a parton state in the above equation. Note that the renormalized fragmentation functions $D_i^j(z_h, \mu)$ at NLO in the $\overline{\mathrm{MS}}$ scheme are given by

$$D_i^j(z_h, \mu) = \delta_{ij}\delta(1-z_h) + \frac{\alpha_s}{2\pi}P_{ji}(z_h)\left(-\frac{1}{\epsilon}\right). \quad (82)$$

With these results at hand and using the expressions for $\mathcal{G}_i^j(z, z_h, E_J, \mu)$ from the previous section, one can obtain the matching coefficient functions $\mathcal{J}_{ij}$, which are free of any divergences. For the maximized jet algorithm, they can be expressed as follows:

$$\begin{aligned}\mathcal{J}_{qq}(z, z_h, E_J, \mu) = {}& \delta(1-z)\delta(1-z_h) + \frac{\alpha_s}{2\pi}\bigg\{L[P_{qq}(z)\delta(1-z_h) - P_{qq}(z_h)\delta(1-z)] \\ & + \delta(1-z)\left[2C_F(1+z_h^2)\left(\frac{\ln(1-z_h)}{1-z_h}\right)_+ + C_F(1-z_h) + \mathcal{I}_{qq}^{\mathrm{alg}}(z_h)\right] \\ & - \delta(1-z_h)\left[2C_F(1+z^2)\left(\frac{\ln(1-z)}{1-z}\right)_+ + C_F(1-z) + \mathcal{I}_{qq}^{\prime\mathrm{alg}}(z)\right]\bigg\}, \end{aligned} \quad (83)$$

$$\begin{aligned}\mathcal{J}_{gg}(z, z_h, E_J, \mu) = {}& \delta(1-z)\delta(1-z_h) + \frac{\alpha_s}{2\pi}\bigg\{L[P_{gg}(z)\delta(1-z_h) - P_{gg}(z_h)\delta(1-z)] \\ & + \delta(1-z)\left[4C_A\frac{(1-z_h+z_h^2)^2}{z_h}\left(\frac{\ln(1-z_h)}{1-z_h}\right)_+ + \mathcal{I}_{gg}^{\mathrm{alg}}(z_h)\right] \\ & - \delta(1-z_h)\left[4C_A\frac{(1-z+z^2)^2}{z}\left(\frac{\ln(1-z)}{1-z}\right)_+ + \mathcal{I}_{gg}^{\prime\mathrm{alg}}(z)\right]\bigg\}, \end{aligned} \quad (84)$$

$$\begin{aligned}\mathcal{J}_{qg}(z, z_h, E_J, \mu) = {}& \frac{\alpha_s}{2\pi}\{L[P_{gq}(z)\delta(1-z_h) - P_{gq}(z_h)\delta(1-z)] + \delta(1-z)[2P_{gq}(z_h)\ln(1-z_h) + C_F z_h + \mathcal{I}_{qg}^{\mathrm{alg}}(z_h)] \\ & - \delta(1-z_h)[2P_{gq}(z)\ln(1-z) + C_F z + \mathcal{I}_{qg}^{\prime\mathrm{alg}}(z)]\}, \end{aligned} \quad (85)$$

$$\mathcal{J}_{gq}(z,z_h,E_J,\mu)=\frac{\alpha_s}{2\pi}\{L[P_{qg}(z)\delta(1-z_h)-P_{qg}(z_h)\delta(1-z)]+\delta(1-z)[2P_{qg}(z_h)\ln(1-z_h)+2T_F z_h(1-z_h)+\mathcal{I}^{\mathrm{alg}}_{gq}(z_h)] \\ -\delta(1-z_h)[2P_{qg}(z)\ln(1-z)+2T_F z(1-z)+\mathcal{I}'^{\mathrm{alg}}_{gq}(z)]\}, \quad (86)$$

where $\mathcal{I}^{\mathrm{alg}}_{ij}(z_h)$ and $\mathcal{I}'^{\mathrm{alg}}_{ij}(z_h)$ are algorithm-dependent functions with the following expressions for the $J^{(I)}_{E_T}$ and $J^{(II)}_{E_T}$ algorithms:

$$\mathcal{I}^{(I)}_{ij}(z_h)=P_{ji}(z_h)\ln z_h+\Theta(1/2-z_h)P_{ji}(z_h)\ln\left(\frac{z_h}{1-z_h}\right), \quad (87)$$

$$\mathcal{I}^{(II)}_{ij}(z_h)=\tilde{P}_{ji}(z_h)\ln(z_h(1+z_h)) \\ +\Theta(1/2-z_h)P_{ji}(z_h)\ln\left(\frac{z_h(2-z_h)}{1-z_h^2}\right), \quad (88)$$

$$\mathcal{I}'^{(I)}_{ij}(z)=-\Theta(1/2-z)P_{ji}(z)\ln\left(\frac{1-z}{z}\right), \quad (89)$$

$$\mathcal{I}'^{(II)}_{ij}(z)=\tilde{P}_{ji}(z)\ln(1+z) \\ +\Theta(1/2-z)P_{ji}(z)\ln\left(\frac{z(2-z)}{1-z^2}\right). \quad (90)$$

Similar to the standard collinear fragmentation functions, the SIFJFs satisfy the momentum sum rules [55,56]. These can be represented by the relations between the SIJFs and the SIFJFs:

$$\int_0^1 dz_h z_h[\mathcal{G}^q_q(z,z_h,E_J,\mu)+\mathcal{G}^g_q(z,z_h,E_J,\mu)]=J_q(z,E_J,\mu), \quad (91)$$

$$\int_0^1 dz_h z_h[\mathcal{G}^g_g(z,z_h,E_J,\mu)+2n_f\mathcal{G}^q_g(z,z_h,E_J,\mu)]=J_g(z,E_J,\mu). \quad (92)$$

Equivalently, we have

$$\int_0^1 dz_h z_h[\mathcal{J}_{qq}(z,z_h,E_J,\mu)+\mathcal{J}_{qg}(z,z_h,E_J,\mu)]=J_q(z,E_J,\mu), \quad (93)$$

$$\int_0^1 dz_h z_h[\mathcal{J}_{gg}(z,z_h,E_J,\mu)+2n_f\mathcal{J}_{gq}(z,z_h,E_J,\mu)]=J_g(z,E_J,\mu). \quad (94)$$

The above two equations provide us a good way to double check our final results. We have checked for both $J^{(I)}_{E_T}$ and $J^{(II)}_{E_T}$ algorithms that our results satisfy the above momentum sum rules. It is instructive to emphasize again the important role of these momentum sum rules in obtaining the correct results for SIFJFs. The correct jet algorithm constraint in Eq. (26) is again crucial. Note that the result for the $J^{(I)}_{E_T}$ algorithm has first been derived from the standard pQCD method in Ref. [27]. Again, our results are slightly different from those in the originally published version of Ref. [27] but are consistent with its updated version. On the other hand, the results of the SIFJFs for the $J^{(II)}_{E_T}$ algorithm are written down here for the first time as far as we know.

V. CONCLUSION

In this paper, we evaluated the semi-inclusive jet functions and semi-inclusive fragmenting jet functions at next-to-leading order, for both quark and gluon jets in the so-called maximized jet algorithms $J^{(I)}_{E_T}$ and $J^{(II)}_{E_T}$ within the framework of soft-collinear effective theory. We started from the operator definitions for both SIJFs and SIFJFs within SCET, and we checked our results using the corresponding momentum sum rules satisfied by these functions. We compared our fixed-order results with the NLO results using standard pQCD techniques when available, in which we emphasized the important role played by the momentum sum rules. While there were previous calculations for the $J^{(I)}_{E_T}$ algorithm, our results for semi-inclusive fragmenting jet functions for the $J^{(II)}_{E_T}$ algorithm are new. We further derived the renormalization group equations for both the SIJFs and SIFJFs and found that they follow the timelike DGLAP evolution equations, just like the usual collinear fragmentation functions. These maximized jet algorithms contain a parameter β, which controls the geometric size of the reconstructed jet. $\beta \gg 1$ corresponds to a highly collimated jet, very similar to the situation for jets with a very small jet radius R. By solving the renormalization equations and evolving those jet functions from their natural scale to the typical hard scale, one can then achieve the resummation of the single logarithms of the jet parameter β. In addition, we find that the evolution equations can further resum $\ln z$, where z is the momentum fraction of the parton that initiates the jet carried by the jet itself. Phenomenological implementations of our results to hadronic collisions will be left for future publications. We expect important impact of our results in probing fundamental properties of nuclear medium and hadron fragmentation functions, as pointed out already from other fixed-order calculations; see, for example, Ref. [27].

ACKNOWLEDGMENTS

We thank Werner Vogelsang for very useful comments and communications. H. X. is supported by Guangdong Major Project of Basic and Applied Basic Research No. 2020B0301030008 and by National Science Foundation of China (NSFC) of China under Projects No. 12022512 and No. 12035007, L. W. and B. Z. are supported by the NSFC of China under Project No. 11805167, and Z. K. is supported by the National Science Foundation in the United States under Grants No. PHY-1720486 and No. PHY-1945471.

[1] G. F. Sterman and S. Weinberg, Phys. Rev. Lett. **39**, 1436 (1977).
[2] S. D. Ellis, J. Huston, K. Hatakeyama, P. Loch, and M. Tonnesmann, Prog. Part. Nucl. Phys. **60**, 484 (2008).
[3] S. Sapeta, Prog. Part. Nucl. Phys. **89**, 1 (2016).
[4] C. Buttar *et al.*, Standard Model Handles and Candles Working Group: Tools and Jets Summary Report, in Physics at TeV colliders, La Physique du TeV aux Collisionneurs, Les Houches 2007, 2007 (2008), pp. 121–214 [arXiv:0803.0678].
[5] G. P. Salam, Eur. Phys. J. C **67**, 637 (2010).
[6] A. Altheimer *et al.*, J. Phys. G **39**, 063001 (2012).
[7] H. L. Lai, J. Huston, S. Kuhlmann, F. Olness, J. Owens, D. Soper, W. K. Tung, and H. Weerts, Phys. Rev. D **55**, 1280 (1997).
[8] A. D. Martin, R. G. Roberts, W. J. Stirling, and R. S. Thorne, Eur. Phys. J. C **23**, 73 (2002).
[9] E.-C. Aschenauer, K. Lee, B. S. Page, and F. Ringer, Phys. Rev. D **101**, 054028 (2020).
[10] M. Arratia, Y. Song, F. Ringer, and B. Jacak, Phys. Rev. C **101**, 065204 (2020).
[11] D. Stump, J. Huston, J. Pumplin, W.-K. Tung, H.-L. Lai, S. Kuhlmann, and J. F. Owens, J. High Energy Phys. 10 (2003) 046.
[12] J. M. Butterworth, A. R. Davison, M. Rubin, and G. P. Salam, Phys. Rev. Lett. **100**, 242001 (2008).
[13] I. Vitev, S. Wicks, and B.-W. Zhang, J. High Energy Phys. 11 (2008) 093.
[14] I. Vitev and B.-W. Zhang, Phys. Rev. Lett. **104**, 132001 (2010).
[15] B. Muller, J. Schukraft, and B. Wyslouch, Annu. Rev. Nucl. Part. Sci. **62**, 361 (2012).
[16] N. Armesto and E. Scomparin, Eur. Phys. J. Plus **131**, 52 (2016).
[17] M. Connors, C. Nattrass, R. Reed, and S. Salur, Rev. Mod. Phys. **90**, 025005 (2018).
[18] A. J. Larkoski, I. Moult, and B. Nachman, Phys. Rep. **841**, 1 (2020).
[19] *Quark-Gluon Plasma 5*, edited by X.-N. Wang (World Scientific, New Jersey, 2016).
[20] B. S. Page, X. Chu, and E. C. Aschenauer, Phys. Rev. D **101**, 072003 (2020).
[21] C. W. Bauer, S. Fleming, and M. E. Luke, Phys. Rev. D **63**, 014006 (2000).
[22] C. W. Bauer, S. Fleming, D. Pirjol, and I. W. Stewart, Phys. Rev. D **63**, 114020 (2001).
[23] C. W. Bauer and I. W. Stewart, Phys. Lett. B **516**, 134 (2001).
[24] C. W. Bauer, D. Pirjol, and I. W. Stewart, Phys. Rev. D **65**, 054022 (2002).
[25] Z.-B. Kang, F. Ringer, and I. Vitev, J. High Energy Phys. 10 (2016) 125.
[26] L. Dai, C. Kim, and A. K. Leibovich, Phys. Rev. D **94**, 114023 (2016).
[27] T. Kaufmann, A. Mukherjee, and W. Vogelsang, Phys. Rev. D **92**, 054015 (2015); **101**, 079901(E) (2020).
[28] Z.-B. Kang, F. Ringer, and I. Vitev, J. High Energy Phys. 11 (2016) 155.
[29] Z.-B. Kang, F. Ringer, and I. Vitev, Phys. Lett. B **769**, 242 (2017).
[30] M. Fickinger, S. Fleming, C. Kim, and E. Mereghetti, J. High Energy Phys. 11 (2016) 095.
[31] L. Dai, C. Kim, and A. K. Leibovich, J. High Energy Phys. 09 (2018) 109.
[32] H. T. Li and I. Vitev, J. High Energy Phys. 07 (2019) 148.
[33] Z.-B. Kang, J.-W. Qiu, F. Ringer, H. Xing, and H. Zhang, Phys. Rev. Lett. **119**, 032001 (2017).
[34] R. Bain, L. Dai, A. Leibovich, Y. Makris, and T. Mehen, Phys. Rev. Lett. **119**, 032002 (2017).
[35] M. Dasgupta, F. Dreyer, G. P. Salam, and G. Soyez, J. High Energy Phys. 04 (2015) 039.
[36] H. Georgi, arXiv:1408.1161.
[37] Y. Bai, Z. Han, and R. Lu, J. High Energy Phys. 03 (2015) 102.
[38] T. Kaufmann, A. Mukherjee, and W. Vogelsang, Phys. Rev. D **91**, 034001 (2015); **101**, 079902(E) (2020).
[39] J. Thaler, Phys. Rev. D **92**, 074001 (2015).
[40] I. W. Stewart, F. J. Tackmann, and W. J. Waalewijn, Phys. Rev. Lett. **105**, 092002 (2010).
[41] J. Thaler and K. Van Tilburg, J. High Energy Phys. 03 (2011) 015.
[42] J. Thaler and K. Van Tilburg, J. High Energy Phys. 02 (2012) 093.
[43] T. T. Jouttenus, I. W. Stewart, F. J. Tackmann, and W. J. Waalewijn, Phys. Rev. D **88**, 054031 (2013).
[44] G. C. Blazey *et al.*, Run II jet physics, in Physics at Run II: QCD and Weak Boson Physics Workshop: Final General Meeting (2000), pp. 47–77 [arXiv:hep-ex/0005012].

[45] G. P. Salam and G. Soyez, J. High Energy Phys. 05 (2007) 086.

[46] A. Y. Wei, P. Naik, A. W. Harrow, and J. Thaler, Phys. Rev. D **101**, 094015 (2020).

[47] T. Kadowaki and H. Nishimori, Phys. Rev. E **58**, 5355 (1998).

[48] E. Farhi, J. Goldstone, S. Gutmann, and M. Sipser, arXiv: quant-ph/0001106.

[49] S. D. Ellis, C. K. Vermilion, J. R. Walsh, A. Hornig, and C. Lee, J. High Energy Phys. 11 (2010) 101.

[50] S. D. Ellis and D. E. Soper, Phys. Rev. D **48**, 3160 (1993).

[51] Y. L. Dokshitzer, G. D. Leder, S. Moretti, and B. R. Webber, J. High Energy Phys. 08 (1997) 001.

[52] M. Cacciari, G. P. Salam, and G. Soyez, J. High Energy Phys. 04 (2008) 063.

[53] Z.-B. Kang, F. Ringer, and W. J. Waalewijn, J. High Energy Phys. 07 (2017) 064.

[54] Y. Bai, Z. Han, and R. Lu, arXiv:1509.07522.

[55] M. Procura and I. W. Stewart, Phys. Rev. D **81**, 074009 (2010); **83**, 039902(E) (2011).

[56] M. Procura and W. J. Waalewijn, Phys. Rev. D **85**, 114041 (2012).